Journal of Magnetism and Magnetic Materials 482 (2019) 173–177

Contents lists available at ScienceDirect

Journal of Magnetism and Magnetic Materials

journal homepage: www.elsevier.com/locate/jmmm

Research articles

Free and itinerant electron channels in magnetic NiCu alloys

Z.Z. Li[a,1], W.H. Qi[a,1], L. Ma[a], G.D. Tang[a,b,*], G.H. Wu[b], F.X. Hu[b]

[a] Hebei Advanced Thin Film Laboratory, Department of Physics, Hebei Normal University, Shijiazhuang City 050024, People's Republic of China
[b] State Key Laboratory of Magnetism, Institute of Physics, Chinese Academy of Sciences, Beijing 100190, People's Republic of China

ABSTRACT

The temperature dependence of the resistivity of magnetic NiCu alloys was fitted using an equivalent circuit containing free electron (FE) and itinerant electron (IE) channels. The spin-independent FEs, which moved within a crystal lattice potential field, were not restrained by the electronic orbitals of any ions. The IEs were restrained by the outer electronic orbitals of the ions and could transit with a certain probability between adjacent ions. Below Curie temperature, T_C, the electrical transport of the IEs was spin-dependent. The variation in the T_C of the NiCu alloys as a function of the Cu content was fitted using the Weiss electron pair model. We therefore provided a scheme to explain both electrical transport and magnetic properties using valence electron structure.

1. Introduction

Three models were reviewed previously [1], including an O 2p itinerant electron model for magnetic oxides (IEO model) [2], a new itinerant electron model for magnetic metals (IEM model) [3], and a Weiss electron pair model (WEP model) used to explain the origin of the magnetic ordering energy in magnetic metals and oxides [4]. These new phenomenological models are based on atomic physics and are easier to understand compared with the conventional exchange interaction models [5]. The new models can be applied to suitable materials to successfully explain the experimental phenomena, including not only those that have been explained using conventional models but also those that have not been explained for many years [1]. The success of these new models implies that the conventional models should be improved or updated.

The IEM model [1,3] is based on the experimental results of the electron transfer from the 4s to the 3d orbital in Fe single crystals [6] and Fe clusters [7]. It includes three postulates: (i) In the process of forming a magnetic metal solid from free 3d transition-metal atoms, most 4s electrons enter the 3d orbitals subjected to Pauli repulsive forces, whereas the remaining 4s electrons form free electrons (FEs). (ii) The 3d electrons located near the Fermi energy level have a certain probability of transiting between the outer electronic orbitals of adjacent ions (i.e., atoms that have lost their FEs) with a constant spin direction, forming itinerant electrons (IEs). The other 3d electrons are local electrons (LEs) belonging to each ion. (iii) FEs moved within a crystal lattice potential field and were not restrained by the electronic orbitals of any ions. Therefore, the movement of FEs is spin-independent. The transition of IEs was restrained by the outer electronic orbitals of the ions. Therefore, the transition of IEs is spin-dependent below the Curie temperature, T_C, but is spin-independent above T_C.

The WEP model [1,4] includes the following assumptions: (i) Two electrons with opposite spin directions in the outer electronic orbital of an ion are assumed to have constant spin directions constrained by Hund's rules [5]. The electrons in the outer electronic orbitals of adjacent ions, including the cations and anions in a compound and the ions in metals, may have three states as shown in Fig. 1. (ii) The two meeting electrons shown in Fig. 1 (A), cannot exchange because they have opposite spin directions. This electron pair with a certain probability and lifetime is called a WEP. The energy difference between static magnetic attractive and Pauli repulsive energies for the two electrons of a WEP are presumably the origin of the magnetic ordering energy in magnetic materials. (iii) The two meeting electrons shown in Fig. 1 (B), can easily exchange because they have the same spin direction. If the electrons adopt the state shown in Fig. 1 (C), the middle electron can easily transit to the electronic orbital of the right ion. The exchange process in Fig. 1 (B) and the transit process in Fig. 1 (C) are the transitions of IEs, wherein the spin direction of the IE cannot change; otherwise, the transition does not occur.

The different characteristics of FEs and IEs in a metal or alloy material have not been reported yet. Herein, such differences are described by analyzing the dependences of the observed magnetic moment, μ_{obs}, and the resistivity, ρ, of $Ni_{1-x}Cu_x$ alloys on their Cu content, x. The known magnetic and electrical experimental phenomena [5,8,9] of $Ni_{1-x}Cu_x$ alloys are explained based on the IEM and WEP models.

* Corresponding author at: Hebei Advanced Thin Film Laboratory, Department of Physics, Hebei Normal University, Shijiazhuang City 050024, People's Republic of China.
E-mail address: tanggd@hebtu.edu.cn (G.D. Tang).
[1] These authors (Z. Z. Li, W. H. Qi) made equal contributions.

https://doi.org/10.1016/j.jmmm.2019.03.011
Received 14 January 2019; Received in revised form 14 February 2019; Accepted 4 March 2019
Available online 04 March 2019
0304-8853/

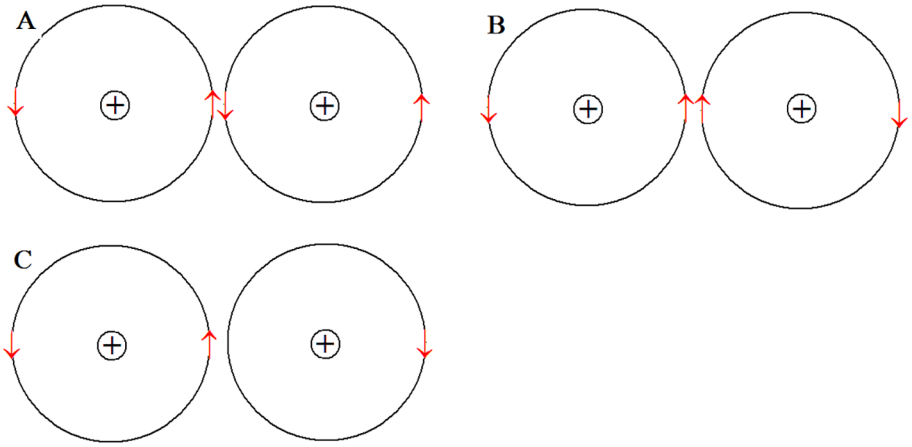

Fig. 1. Illustrations of (A) A Weiss electron pair and (B), (C) itinerant electrons between the outer electronic orbitals of the adjacent ions [1,4].

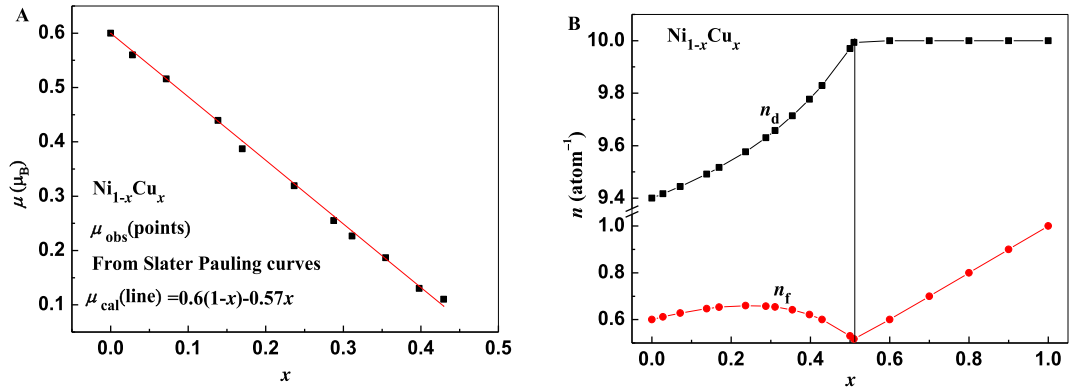

Fig. 2. Studies on $Ni_{1-x}Cu_x$ alloys: (A) Dependence of the observed (points) [5] and fitted (line) average magnetic moments per atom on the Cu content x. (B) Dependencies of the average numbers of 3d electrons per Ni ion (n_d) and FEs per atom (n_f) on x.

2. Free and 3d electron content in NiCu alloys

The dependence of the average magnetic moment, μ_{obs}, of $Ni_{1-x}Cu_x$ (per atom of alloy) on the Cu content (x) was derived from Slater–Pauling curves [5], as shown in Fig. 2 (A). This can be fitted to the following equation:

$$\mu_{cal} = 0.6(1 - x) - 0.57x \quad (1)$$

Eq. (1) can be explained according to the IEM model [1,3]: (i) In 10 valence electrons with $3d^84s^2$ configuration per Ni atom, an average of 9.4 electrons enters the 3d orbitals and 0.6 electrons form FEs in the metallic Ni. Therefore, the average magnetic moment per ion in metallic Ni is 0.6 μ_B. (ii) In 11 valence electrons with $3d^{10}4s^1$ configuration per Cu atom, 10 electrons remain in the 3d orbitals of Cu, 0.57 electrons enter the 3d orbitals of the Ni ions in the alloy, and 0.43 electrons contribute to the FEs of the $Ni_{1-x}Cu_x$ alloys. Therefore, the variations in the average numbers of 3d electrons per Ni ion (n_d) and FEs per atom (n_f) in the NiCu alloy as a function of x can be calculated using the following equations:

$$n_d = 9.40 + \frac{0.57x}{1 - x}, \quad (n_d \leqslant 10.0) \quad (2)$$

$$n_f = 10 + x - n_d \quad (3)$$

Fig. 2 (B) shows the dependencies of n_d and n_f on x. Since the n_d value increases to 10.0 for a full 3d electron shell when $x = 0.51$, we obtain an interesting result: $n_d = 10.0$, $n_f = x$, when $x > 0.51$. This result will be useful for explaining the experimental observations of the electrical-transport properties described below.

3. Electrical-transport model with FE and IE channels

Fig. 3 depicts the curves of resistivity (ρ) versus test temperature (T) and Cu content (x) for the $Ni_{1-x}Cu_x$ alloys reported in Ref. [8], where both x and T_C are shown. These curves are discussed as follows:

(i) For materials with $x = 0.00$, 0.0961, 0.1954, and 0.2810, the T_C is within the test temperature range. Below T_C, ρ increases rapidly with increasing T, whereas above T_C, ρ increases steadily. The dependence of ρ on T can be fitted using an equivalent device with two current-carrier channels, as shown in Fig. 4. Therein, R_3 represents the resistance (resistivity ρ_3) originated from the FEs, which are scattered by a weak, periodic crystal-lattice potential field. R_1 represents the resistance (resistivity ρ_1) originated from the transition of IEs between adjacent ions, which are scattered by the crystal lattice. R_2 represents the resistance (resistivity ρ_2) originated from the IEs, whose spin direction deviates rapidly from the ground-state direction when T is close to T_C. Therefore, the total resistance, R, in Fig. 4, can be calculated using the equation

$$\frac{1}{R} = \frac{1}{R_3} + \frac{1}{R_1 + R_2}$$

and

$$R = \frac{(R_1 + R_2)R_3}{R_1 + R_2 + R_3}$$

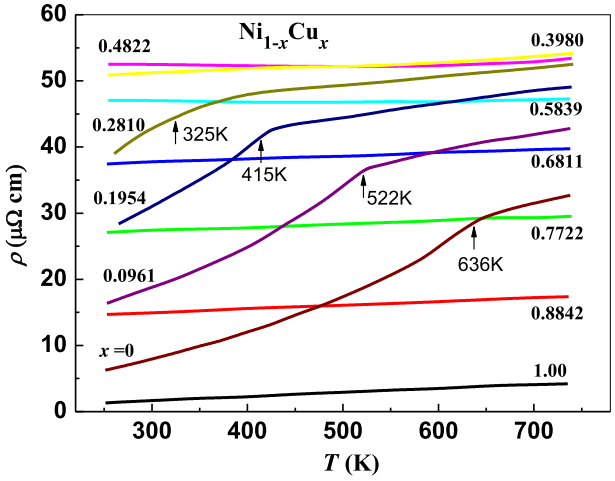

Fig. 3. Resistivity (ρ) versus test temperature (T) and Cu content (x) in $Ni_{1-x}Cu_x$ alloys. The values of x and the Curie temperature, T_C, are shown. The data were taken from Ref. [8].

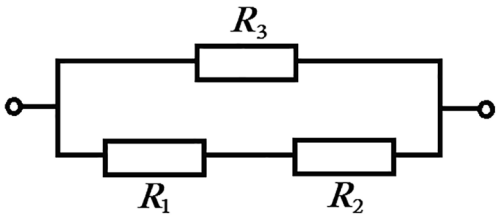

Fig. 4. An equivalent circuit with two current-carrier channels, used to fit the dependencies of ρ on T for a magnetic metal or alloy, where R_3 is in the channel of the FEs, and R_1 and R_2 are in the channel of the IEs.

Thus, the resistivity, ρ, of the materials can be calculated using Eq. (4):

$$\rho = \frac{(\rho_1 + \rho_2)\rho_3}{\rho_1 + \rho_2 + \rho_3} \tag{4}$$

where the resistivity is given by

$$\rho_1 = 1/\sigma_1,\ \rho_2 = 1/\sigma_2,\ \rho_3 = 1/\sigma_3, \tag{5}$$

and the conductivity is given by

$$\sigma_1 = (a_{11} - a_{12}T)^3,$$
$$\sigma_2 = a_2 \exp\left(\frac{E}{k_B T}\right),$$
$$\sigma_3 = \sigma_0 - a_3 T \tag{6}$$

The fitted results obtained using Eqs. (4)–(6) for metallic Ni are shown in Fig. 5, where the points represent previously derived data [8] and the curves represent the fitted results. Thus, (a) if $T \ll T_C$, ρ_2 is very small; $\rho_1 < \rho_3$, and the electrical transport occurs along both channels. (b) With increasing T, the effects of crystal-lattice vibrations on ρ_1 become much stronger than those on ρ_3; therefore, ρ_1 increases faster with increasing T compared to ρ_3. (c) If T is close to T_C, ρ_2 increases rapidly. (d) If $T > T_C$, both ρ_1 and ρ_2 are much higher than ρ_3; the electrical transport occurs along the FE channel; and the contribution of the IEs to the conductivity can be neglected.

(ii) Fitted results of the dependence of ρ on T for materials with $x = 0.00$, 0.0961, 0.1954, and 0.2810 are shown in Fig. 6. The fitted results (curves) are very close to the observed data points [8]. The fitted parameters in Eq. (6) are listed in Table 1. The parameters a_{11} and a_{12} are corresponding to the effect of crystal lattice vibration on spin-dependent transition of IEs. The parameter a_2 is corresponding to the effect of the spin direction of IEs because it deviates from the ground-state spin direction when the test temperature increases. The parameters σ_0 and a_3 are corresponding to the effect on FEs of periodic crystal-lattice potential field. These effects are related to x.

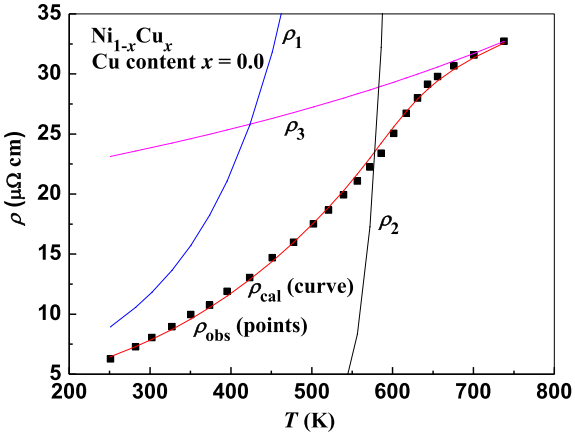

Fig. 5. Illustration of the fitted resistivity curves, ρ_1, ρ_2, ρ_3, and ρ, versus the temperature, T, for the magnetic metal Ni. The observed point data were taken from Ref. [8].

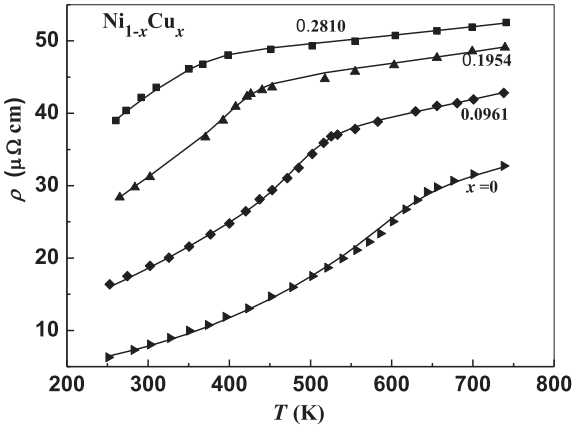

Fig. 6. Fitted resistivity (ρ) curves versus test temperature (T) for $Ni_{1-x}Cu_x$ alloys. The point data were taken from Ref. [8].

When $x \leq 0.281$, an increase in total resistivity, ρ, is observed, which originates from a decrease in σ_0 with increasing x. This may result from two factors: the effect of the crystal-lattice potential field increases due to the increase in Cu content and the concentration of FEs changes slightly [Fig. 2 (B)]. When $x > 0.5$, a decrease in ρ is observed (Fig. 3), which may originate from an increase in the concentration of FEs with increasing x, as shown in Fig. 2 (B).

(iii) Interestingly, the dependences of ρ_1 and ρ_2 on T in Eqs. (5) and (6) are very similar to those reported for perovskite manganites [10]. In particular, the thermal excitation energy, E, of the spin-dependent resistivity, ρ_2, decreases with decreasing T_C in the $Ni_{1-x}Cu_x$ alloys (Table 1) or perovskite manganites $La_{1-x}Sr_xMnO_3$ [10], as shown in Fig. 7. This indicates that the assumption, that IEs exhibit similar properties in magnetic alloys and oxides in the WEP model [1,4], is reasonable.

(iv) Notably, there are obvious difference in electrical transport between magnetic metals and oxides below T_C: In magnetic metals or alloys, the current carriers include the spin-independent FEs and

Table 1
Fitted parameters of the conductivity $\sigma_1 = (a_{11} - a_{12}T)^3$, $\sigma_2 = a_2 \exp\left(\frac{E}{k_B T}\right)$, and $\sigma_3 = \sigma_0 - a_3 T$ for $Ni_{1-x}Cu_x$ alloys.

x	a_{11} ($\Omega^{-1/3}cm^{-1/3}$)	a_{12} ($\Omega^{-1/3}$ $cm^{-1/3}$ $K^{-1/3}$)	a_2 ($\Omega^{-1}cm^{-1}$)	E (eV)	T_C (K)	σ_0 ($\Omega^{-1}cm^{-1}$)	a_3 ($\Omega^{-1}cm^{-1}$ K^{-1})
0.00	0.690	8.30×10^{-4}	2.22×10^{-13}	1.30	636	0.04975	2.65×10^{-5}
0.0961	0.470	6.00×10^{-4}	1.82×10^{-13}	1.03	522	0.03365	1.40×10^{-5}
0.1954	0.385	6.00×10^{-4}	1.54×10^{-13}	0.85	415	0.02552	7.00×10^{-6}
0.2810	0.345	7.00×10^{-4}	1.25×10^{-13}	0.75	325	0.02246	4.60×10^{-6}

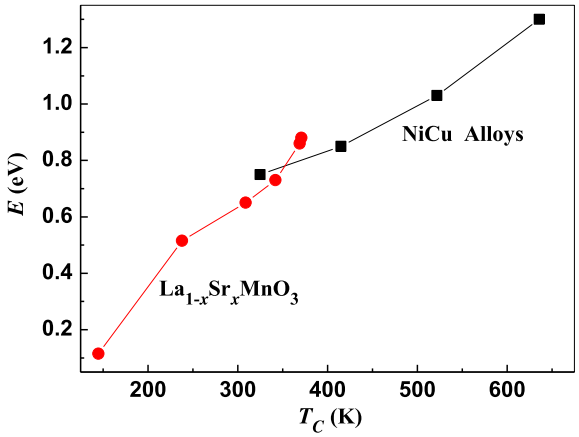

Fig. 7. Thermal excitation energy (E) of the spin-dependent resistivity (ρ_2) versus the Curie temperature (T_C) for the $Ni_{1-x}Cu_x$ alloys studied in this work and the perovskite manganites ($La_{1-x}Sr_xMnO_3$) reported in Ref. [10].

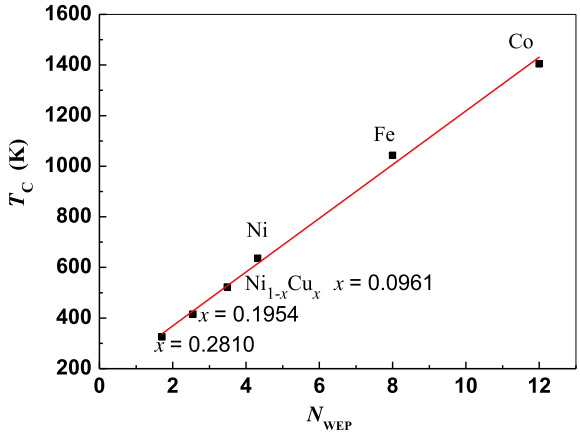

Fig. 8. Dependence of T_C on the average chemical bond number near a magnetic ion, N_{WEP}, at which bonds WEPs can form in a certain probability for $Ni_{1-x}Cu_x$ alloys and Fe and Co metals.

spin-dependent IEs. However, in magnetic oxides $La_{1-x}Sr_xMnO_3$ [10], the current carriers include spin-dependent IEs along the O-Mn-O and spin-independent IEs along the O-La(Sr)-O ion chains, no FE along any ion chain. Therefore, the view that the magnetic oxides (such as perovskite manganites) below T_C possess metal electrical conductivity, should be improved [10].

4. An explanation of the Curie temperature using the WEP model

The T_C of $Ni_{1-x}Cu_x$ alloys and Fe and Co metals decreases with a decrease in the average chemical bond number, N_{WEP}, as shown in Fig. 8, at which bonds WEPs can form in a certain probability [1,11]. According to the WEP model [1,4], there is an energy difference between static magnetic attractive and Pauli repulsive energies for the two electrons of a WEP, which is the energy of a WEP. The energy of WEPs results in decrease of the system energy, and it is assumed to be the origin of the magnetic ordering energy. In the magnetic metal Co, each ion has 12 nearest adjacent ions. In other words, on average, there are 12 bonds near an ion where WEPs can form, represented by $N_{WEP} = 12$. For the magnetic metal Fe, it can similarly be calculated that $N_{WEP} = 8$. Thus, the T_C value for Fe (1043 K) is lower than that for Co (1404 K).

For the magnetic metal Ni, each ion has 12 nearest adjacent ions. The average number of 3d electrons in metallic Ni is 9.40. In other words, 40% of the Ni ions have a full $3d^{10}$ sub-shell with ten 3d electrons being similar to the Cu ions in metallic Cu, which cannot form WEPs with their adjacent ions. Therefore, only 60% of the Ni ions can form WEPs with 60% of their nearest adjacent ions, resulting in $N_{WEP} = 4.32$ ($=12 \times 0.6 \times 0.6$). In the case of $Ni_{1-x}Cu_x$ alloys with $x = 0.0961$, 0.1954, and 0.2810, using the average 3d-electron number, n_d, obtained for Ni ions using Eq. (2), the N_{WEP} values can be calculated to be 3.49, 2.56, and 1.71, respectively. We therefore obtained an approximate linear dependence of T_C on N_{WEP}, as shown in Fig. 8. This indicates that the WEP model, including the assumption that the magnetic ordering energy originates from WEPs, and the IEM model, including the classification of electrons in FEs, IEs, and LEs, are both reasonable.

5. Conclusion

Herein, the dependences of the resistivity and Curie temperature of $Ni_{1-x}Cu_x$ alloys on their Cu content were explained using the IEM and WEP models. The electrical resistivities of the alloys can be fitted using an equivalent circuit with two channels. One channel corresponds to FEs, which have an equivalent resistance R_3. The other channel corresponds to IEs, which have two series of resistances, namely, R_1 (crystal lattice scattering) and R_2 (effect of spin direction below T_C). The relative fitted equations and parameters were presented. The results revealed that T_C of $Ni_{1-x}Cu_x$ alloys and Fe and Co metals decreases with decreasing average chemical bond number, N_{WEP}, at which bonds WEPs can form in a certain probability.

Acknowledgments

This work was supported by the Natural Science Foundation of Hebei Province, China (Grant No. E2015205111), the National Natural Science Foundation of China (Grant No. NSF-11174069), the Young Scholar Science Foundation of the Education Department of Hebei Province, China (Grant No. QN2016015). The authors would like to thank Enago (www.enago.cn) for the English language review.

References

[1] G.D. Tang, Z.Z. Li, L. Ma, W.H. Qi, L.Q. Wu, X.S. Ge, G.H. Wu, F.X. Hu, Phys. Rep. 758 (2018) 1–56.
[2] J. Xu, L. Ma, Z.Z. Li, L.L. Lang, W.H. Qi, G.D. Tang, L.Q. Wu, L.C. Xue, G.H. Wu,

Phys. Status. Solidi. B. 252 (2015) 2820–2829.
[3] W.H. Qi, L. Ma, Z.Z. Li, G.D. Tang, G.H. Wu, Acta Phys. Sin. 66 (2017) 027101(in Chinese with English Abstract).
[4] W.H. Qi, Z.Z. Li, L. Ma, G.D. Tang, G.H. Wu, F.X. Hu, Acta Phys. Sin. 66 (2017) 067501(in Chinese with English Abstract).
[5] C.W. Chen, Magnetism and Metallurgy of Soft Magnetic Materials, North-Holland Publishing Company, 1977, pp. 171–417.
[6] W. Jauch, M. Reehuis, Phys. Rev. B. 76 (2007) 235121.
[7] G.E. Pacchioni, L. Gragnaniello, F. Donati, M. Pivetta, G. Autès, O.V. Yazyev, S. Rusponi, H. Brune, Phys. Rev. B. 91 (2015) 235426.
[8] J.X. Fang, L. Dong, Solid State Physics (in Chinese), Shanghai Scientific and Technical Publishers, 1981, pp. 310–315.
[9] R.W. Houghton, M.P. Sarachik, J.S. Kouvel, Phys. Rev. Lett. 25 (1970) 238–239.
[10] J.J. Qian, W.H. Qi, Z.Z. Li, L. Ma, G.D. Tang, Y.N. Du, M.Y. Chen, G.H. Wu, F.X. Hu, RSC Advances 8 (2018) 4417–4425.
[11] W.H. Qi, Z.Z. Li, L. Ma, G.D. Tang, G.H. Wu, AIP Advances 8 (2018) 065105.